FIRST GLOBAL ANALYSIS OF SEASAT SCATTEROMETER WINDS AND POTENTIAL FOR METEOROLOGICAL RESEARCH

Steven Peteherych
Atmospheric Environment Service, Downsview, Ontario M3H 5T4, Canada
Morton G. Wurtele
Department of Atmospheric Sciences, U.C.L.A., Los Angeles, CA 90024, USA
Peter M. Woiceshyn
Jet Propulsion Laboratory/California Institute of Technology, Pasadena, CA 91109, USA
Dale H. Boggs
dB Systems, Ltd., Inc., La Canada-Flintridge, CA 91011, USA
Robert R. Atlas
Goddard Laboratory of Atmospheric Sciences/NASA, Greenbelt, MD 20771, USA

1. ABSTRACT

The first global wind fields from Seasat scatterometer data have now been produced. Fifteen days (Sept. 6-20, 1978) of record are available on tape, with unique wind directions indicated for each observation. The methodology of the production of this data set is described, as well as the testing of its validity. A number of displays of the data, on large and small scales, analyzed and gridded, are provided.

2. INTRODUCTION

This paper is concerned with the production and scientific potential of global data sets from Seasat Scatterometer (SASS) data record. The validation of the individual wind vector observations is fully documented (Jones et al., 1982; Schroeder et al., 1982) and is here taken as established, although elsewhere in this volume (Woiceshyn et al., 1984), certain features of the geophysical algorithm are called into question. A number of interesting case studied using SASS data have demonstrated the capability of revolving features and patterns with significantly greater accuracy and resolution than is possible with conventional data (Peterych et al., 1981; Pierson, Sylvester, and Salfi, 1984). However, the problems associated with the production of a global data sets, and the research made possible through use of such sets, are different from those involved in case studies; and these aspects of SASS data are the ones treated herein.

As is well known, the Seasat Scatterometer, having two antennas on each side, produced a Geophysical Data Record (GDR) that is ambiguous as to wind direction, with two to four alternative directions associated with each pair of doppler cells. Figure 1 displays schematically the relation between the number and orientation of alternative wind directions and the direction of the satellite antennas. This relationship became crucial in the methodology of producing a set of unique wind vectors from the SASS data, as will be seen below.

Two major field programs, the Gulf of Alaska Experiment (GOASEX) and the Joint Air-Sea Interaction Experiment (JASIN) in the northeast Atlantic provided observational data against which the Seasat geophysical data, including those from SASS, could be compared and validated. The comparisons were carried out in three workshops organized for that purpose.

The process of selecting a single direction from among alternatives ("aliases") became known as "dealiasing," and partial regional data sets were dealised for the GOASEX and JASIN workshops. It was evident to meteorologists

that dealising could be achieved by that process of subjective pattern-recognition that is called meteorological analysis; and this procedure, as well as the SASS technology in producing wind measurements, was validated at the two workshops. The GOASEX workshop results were reported by Jones et al. (1979). The cover of the issue of Science containing the GOASEX reports was devoted to a dealised SASS swath off the Canada/Alaska coast. since that publication date, all available ship observations were collected and added to the figure to show the near-perfect agreement. This is here reproduced as Figure 2, with the ship winds drafted in heavier line than the SASS winds.

In the case of JASIN, two teams of analysts worked independently and without the aid of in situ observations or satellite imagery. Their final products agreed to an extent that was acceptable to the workshop scientists, and did not require alteration when the in situ data were made available. Details of this experiment are presented in the article by Wurtele et al. (1982), in which the fundamental kinematic patterns - common to all two-dimensional vector fields -- are systematically described, and examples given illustrating the realization of these patterns in JASIN data.
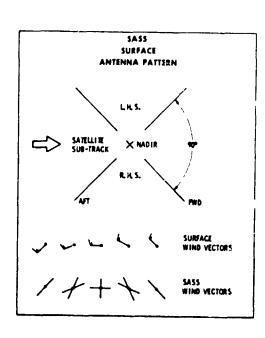

Figure 1. Schematic showing relation between wind direction antenna orientation, and SASS reported directions.

Figure 2. SASS Rev 1140 from GOASEX workshop, dealiased, with satellite imagery superimposed. Note 50-km resolution. Ship-observed winds have been added in heavy line drafting to compare with scatterometer data.

3. PRODUCTION OF THE DATA FILE

In July 1982 a cooperative project was begun to dealise a global data set. The participating institutions were Jet Propulsion Laboratory, Atmospheric Environment Service ol Canada (AES), NASA Goddard, and U.C.L.A. (Meanwhile, objective dealiasing techniques had been under investigation at Goddard Laboratory of Atmospheric Science (Baker et al., 1984), and the two methodologies contributed to the development of each other.)

The official GDR was found less useful in the subjective dealising than the charts produced by ⌐ES, on which the SASS observation were plotted with 100 km-resolution at equal intervals and in rows normal to the satellite subtrack. In situ data from coastal stations and ships were plotted on charts with identical cartography. The aralysts consulted also imagery from GOES East and West, DMSP, and Meteosat. (In fact, the analysts were quickly impressed by the extent to which the cloud patterns – at any height – could be associated with surface wind patterns.)

As with JASIN, the analysts worked in two teams, independently, one at AES, the other with JPL/UCLA. Various measures were recorded of the agreement of the wind-vector selections of the two teams; here it suffices to say that agreement without consultation was achieved in about 80 percent of the individual vectors. The areas of disagreement were discussed in workshops, and a "consensus" set of selected wind vectors was determined.

At this point, however, a severe data-handling problem arose, that had not been faced with the GOASEX and JASIN data. When the analysts had done their work, the consensus data existed only on the analysts' charts; it now had to become a part of the SASS data tape, that each SASS wind observation would have one of its alternatives designated as the "correct" direction. Each chart contained approximately 4500 wind observations, and each SASS-day required six charts.

The procedure finally adopted for this massive data handling constituted a semi-automated routine based on the characteristics of the SASS instrument represented in Figure 1. There, it will be noted, the true direction varies by no more than 90 degrees, and each SASS datum has one and only one direction in that quadrant. Thus a single designator, for the rear quadrant, can specify the correct selection from the aliases. Thus it is possible to delineate polygonal areas within a SASS swath – greater or lesser in extent – within which all "correct" wind directions fall within a single quadrant, relative to the satellite sub-track. The vertices of these polygons are identified and recorded on tape by a digitizer, together with the essential information, including, of course, the quadrant direction designator. An example of five SASS swaths divided among polygons is presented in Figure 3. The polygon file thus generated is merged with the original SASS data file to create a geophysical data record of unique marine wind vectors. (The alias directions are retained in the file for the benefit of scientists who prefer to do it themselves).

**QUADRANT POLYGONS DEFINING REGIONS AND
DIRECTIONS FOR CREATING DATA RECORD OF UNIQUE
SASS WIND DIRECTIONS BY BATCH PROCESSING**

QUADRANT POLYGON
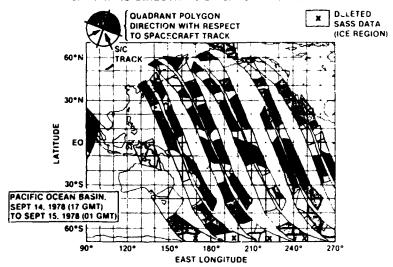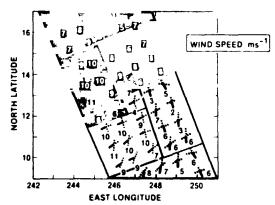DIRECTION WITH RESPECT
TO SPACECRAFT TRACK

DELETED
SASS DATA
(ICE REGION)

S/C
TRACK

60°N

30°N

EQ

LATITUDE

30°S

PACIFIC OCEAN BASIN.
SEPT 14, 1978 (17 GMT)
TO SEPT 15, 1978 (01 GMT)

60°S

90°   120°   150°   180°   210°   240°   270°

EAST LONGITUDE

**DETAIL OF QUADRANT POLYGONS WITH SELECTED
WIND DIRECTION (BLACK)**

16

WIND SPEED ms⁻¹

NORTH LATITUDE

14

12

10

242   244   246   248   250

EAST LONGITUDE

Figure 3. Polygons
indicating wind
direction for five SASS
swaths.

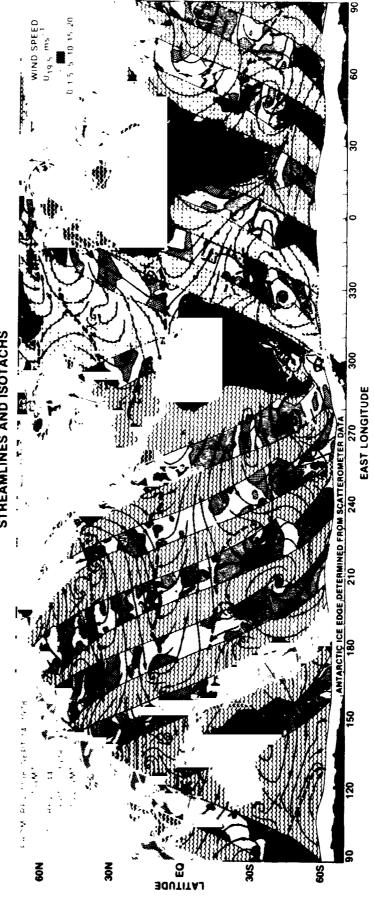# SEASAT SCATTEROMETER GLOBAL MARINE WIND ANALYSIS

STREAMLINES AND ISOTACHS

Figure 4. One global SASS day wind field, represented by streamlines (solid black, with arrows) and isotachs (code at upper right). ITCZ is heavy dashed line; fronts are light dashed lines. Wavy lines designate ocean between SASS swaths.

4. GLOBAL DATA PRESENTATION

By the methods described, then, a total of 15 days of global SASS data has been dealiased, and is now available to scientists upon application to NASA Headquarters. Almost one-half million wind observations are recorded in this data set. There are more observations in some regions of the southern oceans than are represented in the total climatological history of these regions before Seasat. Visual presentation of these global data may be made in a number of ways, and we have chosen the following. Half the globe is plotted with descending orbital data, the other half with the corresponding ascending orbital data. Such a plot is presented in Figure 4. It is a mode of presentation unfamiliar to meteorologists accustomed to synoptic charts.

Consecutive parallel orbits are removed by 1.5 hours in time from each other. The two V-shaped configurations, where ascending and descending orbits meet, represent a 12-hour displacement in time. Between successive orbital swaths streamline interpolation is possible, and in any case, analyses may be checked against co-located data 12 hours earlier or later. Interpolation in the V-regions will constitute, in effect, a smoothing over a 12-hour period, and is therefore less reliable as representing momentary directions. The streamlines in Figure 4 are black lines with direction arrows. Speeds (not interpolated between swaths) are indicated according to the code in the upper right.

Such a global presentation, based on some 28,000 observations, is an exciting event to meteorologists. We note the greater wind speeds in the Southern Hemisphere; the monsoonal flow onto the Indian subcontinent and the African continent, east and west coasts; the two typhoons (Irma and Judy) on either side of the Japanese islands. The Antarctic ice is shown in white, the ice-edge itself having been identified from the SASS observations. The Intertropical Convergence Zone (ITCZ) - a heavy dashed bloack line - shows strongly in the eastern half of the Pacific and extends from Africa to Brazil in the Atlantic.

We may now look in higher resolution at one of the interesting features of the map, the ITCZ in the region of 220-260E. Figure 5 presents an analysis of this area, superimposed on the un-dealiased scatterometer observations. The storm-induced perturbations on the ITCZ are clearly delineated in the 100-km resolution
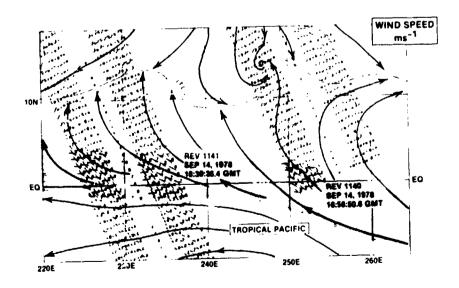

Figure 5. ITCZ area 220-260 E for 14 September.

580

wind data, and even more striking is the different westward flow pattern detected by the SASS data along the Equator, emphasized in the Figure by gray shading. This is not a unique occurrence of this phenomenon. Rather, the data set reveals that when tropical depressions on the ITCZ intensify, they tend to be associated with a zone of divergence along the Equator. The density and quality of the data permit the calculation of vorticity and divergence fields, for the entire global oceans, or for any area of interest. Figures 6 and 7 show, respectively, the contours of vorticity and divergence in the area covered by Figure 5. (Units for both are 10^{-6} s^{-1}). Maxima of vorticity appear at the perturbations of the ITCZ, with values of 4×10^{-5} s^{-1}, and vorticity minima of about half the magnitude, are only four to six degrees to the south. Convergence and divergence maxima, however, are of about equal magnitude ($\pm 3 \times 10^{-5}$ s^{-1}), and are separated by ten degrees latitude, the divergence centers being, as anticipated very near the Equator. These surface flow patterns seem to suggest a meridional circulation, rising over the ITCZ and sinking at the equator.

5. GRIDDED FIELDS

For numerical manipulation, it is essential to connect the streamlines /isotach fields to digital (u,v) vector fields at regularly spaced grid points. This has been done by means of a three-point linear interpolation algorithm modified for the unique requirements of the present project. A display of gridded wind field data is of little interest in itself; but from such fields, with appropriate software, many interesting fields may be derived.

As an example, Figures 8 and 9 present, respectively, the mean eastward and mean northward velocity components for the entire 15-day data set, in the Pacific Ocean. Dashed light contours are for negative values, solid contours for positive, and the heavy solid lines if the zero contour. The huge area of easterly trades dominates Figure 8, with mean westerlies much stronger in the Southern Hemisphere. Figure 9 vividly illustrates the intensity of the ITCZ in the eastern Pacific, and the weakness in the western. Flow onto the Antarctic ice pre- dominates in the Pacific; off the ice, in the Atlantic (not shown). Wind climatologies exist for variety of oceanic regions, and a variety of periods of record. Meteorologists may be impressed to find a 15-day mean so similar in many features to the climatological September. Certainly the question of the time period necessary for averaging out various transient features is an important one in the theory of climate. A systematic discussion would require analysis in terms of impirical orthgonal functions.

Another statistical representation of the data set is contained in Figure 10. Here is contoured the difference between the magnitude of the vector mean wind and the standard deviation of the speed, with positive (dark) and negative areas only being shown for the sake of clarity. Thus a positive area indicates relative steadiness of both direction and speed. An outstanding feature is the steadiness of the Southern Hemisphere belt of westerlies, equally pronounced in Atlantic and Indian Oceans (not shown). Despite the sharp gradients of the north-south component (Figure 9), the region of the ITCZ in Figure 10 is seen to be one in which the standard deviation is greater than the mean, a situation arising from the relative small spatial scale perturbations of the ITCZ. The large positive areas are, of course, the trade wind regions.

Figure 6. Vorticity contours in area of Figure 5. Units: 10^{-6} s^{-1}.
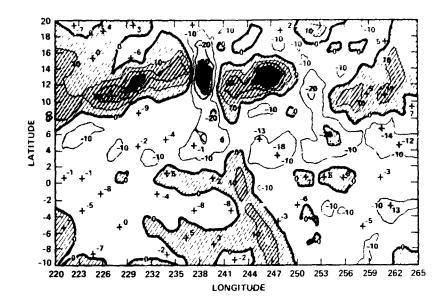

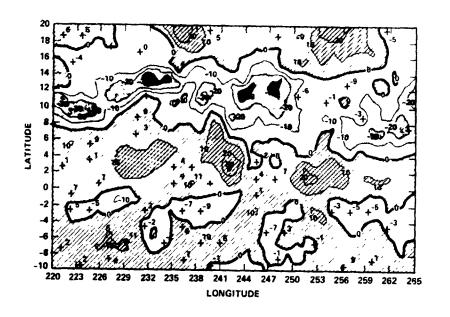Figure 7. Divergence contours in area of Figure 5. Units: 10^{-6} s^{-1}.

Figure 8. Mean west wind
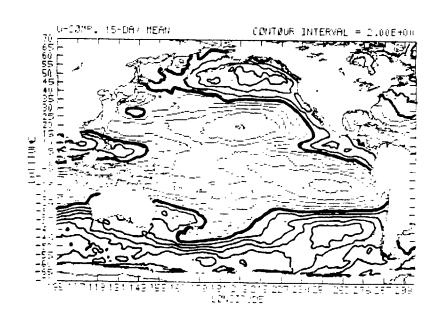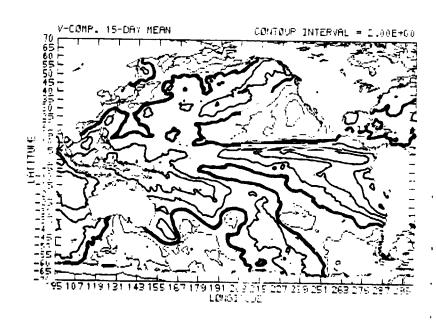component for 15-day data
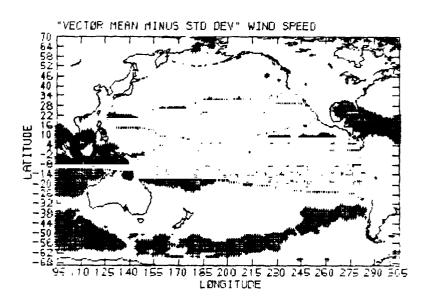set. Solid contours
positive values.

Figure 9. Same as Figure
8 for south wind components.

"VECTOR MEAN MINUS STD DEV" WIND SPEED

Figure 10. Magnitude of vector mean wind minus standard deviation of speed (15-day data set). White areas, positive; shaded areas, negative.

CONCLUSION

Methods have been developed for dealiasing the Seasat SASS data record and for producing a data tape in the same format, but with a unique selected wind direction associated with each observation. Fifteen days (Sept. 6-20, 1978) are now available for scientific use. The resulting global wind fields, as represented by streamlines and isotachs, provide a visualization of meteorological features of every scale upward from 100 km. The data may be interpolated onto a grid array and then handled numerical by conventional procedures.

The scientific opportunities offered by scatterometer data have yet to be systematically discussed, although some areas of especial interest are identified in the forthcoming science opportunities documented for the Navy Remote Oceanographic Satellite System (Freilich, 1984), scheduled for 1988-89 launch.

ACKNOWLEDGMENTS

References

Atlas, R., Petehrych, S., Woiceshyn, P., and Wurtele, M. G., 1982: Analysis of satellite scatterometer data and its impact on weather forecasting, Oceans, September 1982, 415-420.

Baker, W. E., Atlas, R., Kalnay, E., Halem, M., Woiceshyn, P. M., Eddman, D., 1983: Large-scale analysis and forecast experiments with wind data from the Seasat-A scatterometer, to be published, J. Geophys. Res.

Freilich, M., 1984: NROSS Scatterometer Science Opportunities, to be published by JPL, April, 1984.

Hellerman, Sol, and Rosenstein, M., 1983: Normal monthly windstress over the world oceans with error estimates, J. Phys. Ocean., 13, 1093-1104.

Jones, W. L., Black, P. G., Boggs, D. M., Bracalente, E. M., Brown, R. A., Dome, G., Halberstam, I. M., Overland, J. E., Peteherysh, S., Pierson, W. J., Wentz, F. J., Woiceshyn, P. M., and Wurtele, M. G., 1979: Seasat scatterometer results for the Gulf of Alaska Workshop, Science, 204, 1413-1415.

Jones, W. L., Schroeder, L. C., Boggs, D. H., Bracalente, E. N., Brown, R. A., Dome, G. J., Pierson, W. J., and Wentz, F. J., 1982: The Seasat A Satellite Scatterometer: the geophysical evaluation of remotely sensed wind vectors over the oceans, J. Geophys. Res., 87, 3297-3317.

McDonald, W. F., 1938: Atlas of Climatic Charts of the Oceans, U. S. Weather Bureau No. 1247.

Pierson, W. J., Sylvester, W. B., and Salfi, R. E., 1984: Vector wind, horizontal divergence, wind stress curl from Seasat-SASS at a one-degree resolution, These Proceedings.

Peteherych, S., Woiceshyn, P. M., Appleby, W. A., Chu, L., and Spagnol, J., 1981: High resolution marine meteorological analyusis using Seasat data, Oceanography from Space, Plenum Publishing Co., 581-588.

Schroeder, L. E., Boggs, D. H., Dome, G., Halberstam, I. M., Jones, W. L., Pierson, W. J., and Wentz, F. W., 1982: The relationship between wind vector and normalized radar cross section and to derive Seasat A Satllite Scatterometer winds, J. Geophys. Res., 87, 3318-3336.

Woiceshyn, P. M., Wurtele, M. G., McGoldrick, L. F., Boggs, D. H., and Peteherych, S., 1984: A new parameterization of the geophysical processes in wind/ocean scatterometry, these Proceedings.

Wurtele, M. G., Woiceshyn, P. M., Peteherych, S., Borowski, M., and Appleby, W. S., 1982: Wind direction alias removal studies of Seasat Scatterometer-derived winds, J. Geophys. Res., 87, 3365-3377.